Chiang Mai J. Sci. 2005; 32(2) : 109-120
www.science.cmu.ac.th/journal-science/josci.html
Contributed Paper

New Positive Temperature Coefficient Effect Based on Bi_2O_3+Fe_2O_3 or ZrO_2+MnO_2 Material and Used as Temperature Sensor

Thongchai Panmatarith* [a], Chiraporn Sriprom [a] and Nanthida Sutthirawuth [b]
[a] Department of Physics, Faculty of Science, Prince of Songkla University, Hat Yai 90112, Thailand.
[b] Materials Science Field, Faculty of Science, Prince of Songkla University, Hat Yai 90112, Thailand.
*Author for correspondence.

Received : 24 May 2004
Accepted : 1 April 2005

ABSTRACT

The Bi_2O_3+Fe_2O_3 (sample 1) and ZrO_2+MnO_2 (sample 2) materials were prepared by standard ceramic techniques and identified the phase by XRD techniques. The PTC effect was tested. The both samples were applied to be temperature sensor. The sample 1 exhibits PTC effect from 25 to 110 °C that the positive temperature coefficient of the resistance (α) was +183.24 %/°C. The maximum resistance was 22.24 MΩ at 110 °C. The sample 2 exhibits PTC effect from 25 to 130 °C that the positive temperature coefficient of the resistance (α) was +7.08 %/°C. The maximum resistance was 9.08 MΩ at 130 °C. The PTC effect was similar to barium titanate. The PTC effect in the Bi_2O_3+Fe_2O_3 and ZrO_2+MnO_2 samples were discovered in the first time. The prepare samples and the temperature monitoring with computer system can measure the temperature in the range 25 °C to 65 °C (sample 1) and 25 °C to 85 °C (sample 2). The working temperature of these sensors are in the PTC region which are very sensitive to heat.

Keyword : PTC thermistor, temperature sensor.

1. INTRODUCTION

The positive temperature coefficient (PTC) thermistor is the material which can transform temperature change into resistance change [1]. This thermistor shows the semiconducting property. This ceramics is important for industrial work. The well-known PTC thermistors are $BaTiO_3$–based materials which show PTC effect. T_c of $BaTiO_3$ is about 120-130 °C and is changed with dopant content. Dopant is added to $BaTiO_3$ for the changing of potential barrier at grain boundaries. Then the PTC behaviour is changed. This thermistor can be used as temperature sensor, constant temperature heater (PTC heater), honeycomb air heater (hair dryer), auto fuel evaporator, current limiter, circuit timer, sensor for motor protection, motor start assist and high temperature material [2].

PTC thermistor can be operated as thermostat for heat flowing [3]. The $BaTiO_3$+0.4 mol%Ho_2O_3 was prepared and the resistivity, dielectric constant, dissipation factor versus frequency and Curie temperature were measured for PTCR effect studying [4]. The $(Ba_{1-x}Sr_x)(Nb_{0.003}Ti_{0.997})O_3$ + 1 mol% TiO_2+ 0.07 mol% MnO (x=0, 0.2) were prepared in Japan. The electrode was fabricated from silver paste. The resistance versus temperature was measured and applied to be infrared detector [5].

$BaTiO_3$ + 0.3 at% Nb_2O_5 ;$BaTiO_3$ + 0.3 at% Nb_2O_5 + 0.2 at% Bi_2O_3 were prepared in India. The resistivity versus dopant content, the resistivity versus temperature and the dielectric constant versus temperature were measured [6]. $(Sr_{0.2}Ba_{0.8})TiO_3$ was prepared and tested for PTC effect and Curie temperature (T_c) was measured in Taiwan [7]. $(Sr,Pb)TiO_3$ was prepared in China. The resistivity at different temperature and Curie temperature were measured. The PTCR value was calculated [8]. Ca-doped $SrTiO_3$ capacitor was prepared and a was measured in Japan [9]. MnO-doped $BaTiO_3$ was prepared with $Al_2O_3.SiO_2$ as the sintering-aid material and the PTC efficiency was studied in China [10]. The PTCR effect was found in TiO_2-doped $BaNb_2O_6$ in the range 70 to 300 °C in Slowenia [11]. Ho-doped $BaTiO_3$ ceramics was prepared and Curie temperature is at 110 °C in Saudiarabia [12]. PTC effect in the Cr/$(Ba,Pb)TiO_3$ material for overcurrent protection application was reported in Singapore. The structural model was used to explain the PTC effect [13]. The PTC thermistor was found in England and it can be used as overtemperature protectors [14]. The (Y, Mn) co-doped $Sr_{0.5}Pb_{0.5}TiO_3$ thermistors was prepared in China and studied the PTCR effect [15].

$BiFeO_3$ is reported to have both ferroelectric and ferromagnetic natures [16]. $BiFeO_3$ is a perovskite-like compound with magnetic and electrical long-range order with antiferromagnetic transition temperature T_N=670 K [17]. $Bi_4Fe_2O_9$ behaves the magnetic properties in Fe_2O_3-Bi_2O_3 system [18].

$Bi_4Fe_2O_9$ is reported as ferrite material [19]. The gas-sensing characteristics of bismuth ferrites with the compositions $BiFeO_3$, $Bi_4Fe_2O_9$and $Bi_2Fe_4O_9$ as new materials for semiconductor gas sensors are presented [20]. Pure $Bi_2Fe_4O_9$ are reported above and below its magnetic ordering temperature [21].

ZrO_2 is a technologically important material due to its thermal and chemical stability, and excellent mechanical properties, such as high strength and fracture toughness, high melting point, low thermal conductivity, and high corrosion resistance. These unique mechanical and electrical properties of ZrO_2 ceramics have led to their widespread applications in the fields of structural materials, solid-state electrolytes, thermal barriers coatings, electro-optical materials, gas-sensing, corrosion-resistant [22].

Manganese oxides are important materials due to their wide range applications, such as high-density magnetic storage media, catalysts, ion exchange, molecular adsorption, electrochemical materials, varistors and solar energy transformation. One of the manganese oxides, Mn_3O_4 has been widely used as the main source of ferrite materials, which have extensive applications in electronic and imformation technologies. The SQUID results show that Mn_3O_4 nanoparticles exhibit ferromagnetic behaviour, and the magnetization reduces with the decrease of size of the nanoparticles [23].

The PTC effect in Bi_2O_3+Fe_2O_3 and ZrO_2+MnO_2 samples were not reported by anyone. So, the PTC results were not studied. In this study, the Bi_2O_3+Fe_2O_3 and ZrO_2+MnO_2 samples were prepared by the standard ceramic techniques and the sample phases were identified with XRD apparatus. The resistance versus temperature relation of the PTC effect was measured. The PTCR value was calculated. The sample was tested for the temperature sensor.

2. Materials and Methods

2.1 Preparation, Phase Identification and Electroding of the Samples

Samples were measured with standard ceramic techniques as shown in Figure 1 [2]. Sample formulas were selected. Sample 1 and sample 2 were named Bi_2O_3+Fe_2O_3 and ZrO_2+MnO_2, respectively. Sample powders of Bi_2O_3 , Fe_2O_3 ,ZrO_2 and MnO_2 with 99.5% purity were prepared. Sample powders were calculated and weighed. Powders were mixed with mortar and then mixed again by contain the powders in plastic can) and rotate with

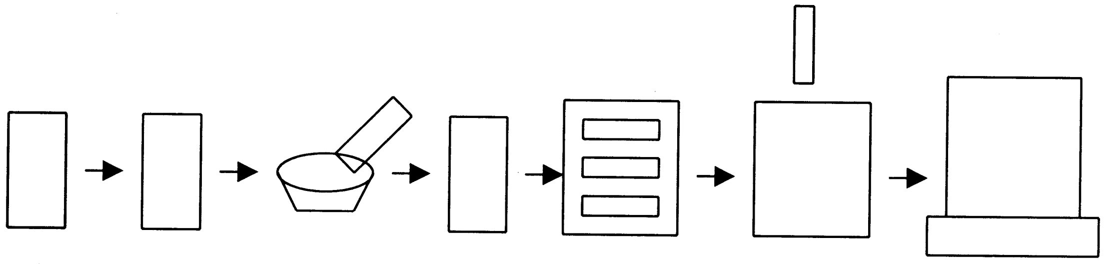

Figure 1. The sample preparation [2].

mixer. PVA (polyvinyl alcohol) and distilled water were added to the powders as a binder for forming granulation. This powders were taken in press mold and were pressed with hydraulic pressor (Rllk 25 tons) into small discs. The one formular is composed of three 3 pellets. The pressed samples were dried for decreasing the sample humidity. The samples were fired with furnace that used temperature controller (FCR-13A-R/M) and type R thermocouple as a temperature sensor. The sample 1 was fired 2 times, the first firing was at 800 °C. The sample 2 was fired 2 times, the first firing was at 550 °C. The second firing of both samples were at 1200 °C. The reason for double firing because the melting point of Bi_2O_3 and MnO_2 are 822 °C and 535 °C, respectively. The second firing was done for atomic movement to form crystal structure. After the first firing, the sample was ground and pressed into the pellets before the second firing. The both samples used a heating rate of 5 °C/min and a soaking time of 1 h. Finally, we obtained the as-fired samples. The prepared samples were identified with XRD apparatus (X-ray diffractometer, Philip PW1730). The sample thickness and diameter were measured with micrometer. The samples were electroded with silver paste by smearing on to the surface, together the pin placing and fired at 120 °C for 20 min.

2.2 PTC Property Measurement

The sample was hold with the stand above the furnace about 0.5 cm for obtaining the proper temperature increasing rate as shown in Figure 2. The resistance (R) was measured with multimeter (Fluke 45) and temperature (T) with temperature apparatus (AVD M890C$^+$). After that the sample

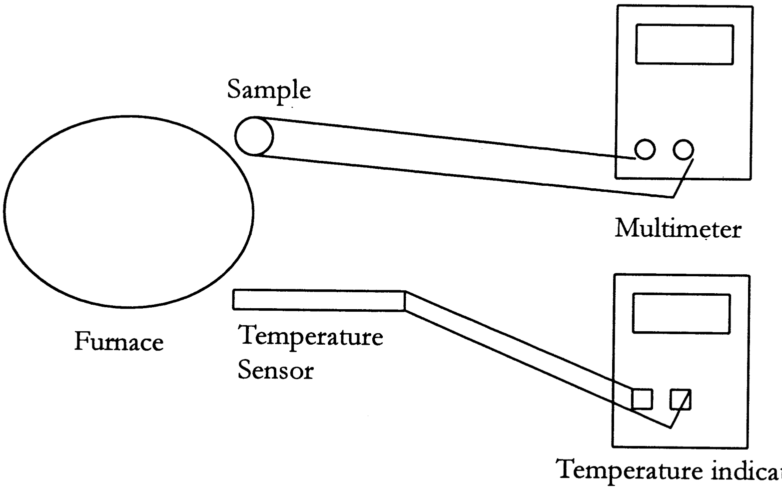

Figure 2. The experimental set up for the resistance versus temperature measurement.

temperature was increased slowly from 25 to 200 oC. The resistance and temperature were recorded and drawn the R vs T graph. The positive temperature coefficient of the resistance was calculated from the formula, $\alpha=(1/R)(dR/dT)$.

2.3 Temperature Sensor Testing

After the sample was measured for the temperature versus temperature relation, the samples were tested as the temperature sensor with the following steps :

1) Computer interfacing system for temperature measurement with the prepared sample as a temperature sensor was designed and constructed as shown in Figure 3. This system is composed of ADC0809, 74LS244, ET-PT8255 Card and computer. After that this circuit was tested for correct operation.

2) Measurement and control program was written and was calibrated for computer reading the temperature with the prepared sample using as a temperature sensor.

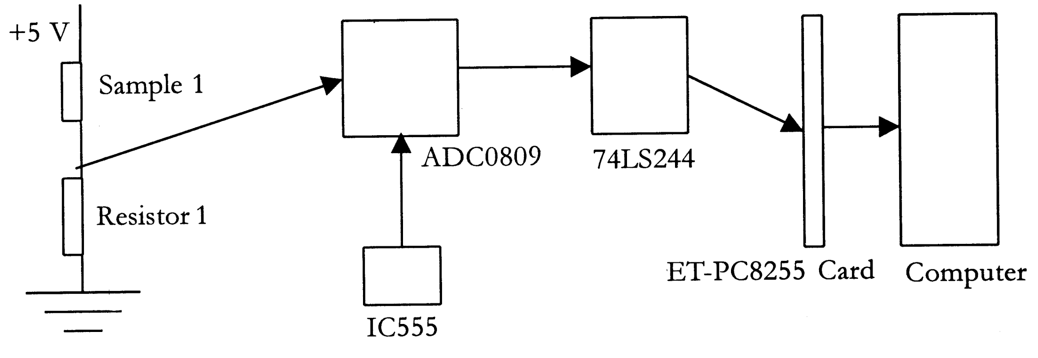

a. The sample 1 (Bi_2O_3+Fe_2O_3)

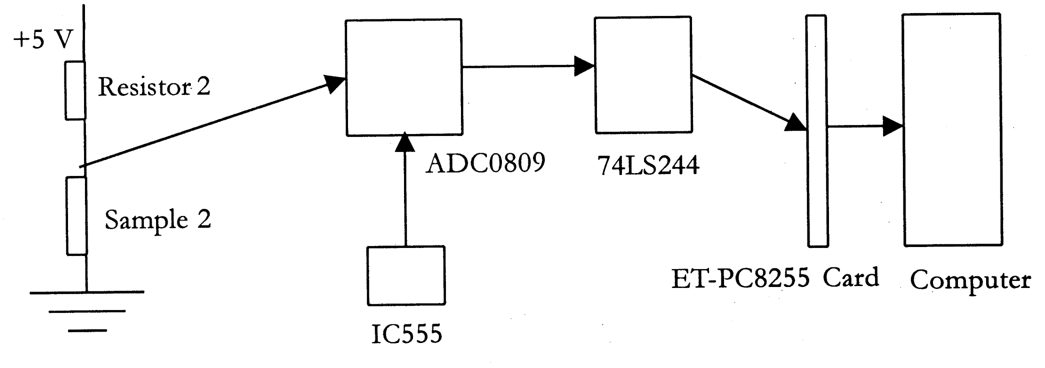

b. The sample 2 (ZrO_2+MnO_2)

Figure 3. Block diagram for temperature measurement system with computer with the prepared sample as a temperature sensor.

```
Program Temperature_Sensor_Testing;
uses   crt ;
var   i, ,j, x, y, DV : integer;
AV, Ttrue : real;
const PA        = $0304;
      Pcontrol = $0307;
begin
  clrscr;
  port[Pcontrol]:=$90;
  gotoxy(25,2); writeln('TEMPERATURE MEASUREMENT');
  gotoxy(25,3); writeln('...............');
  DV := 0 ; AV := 0 ; Ttrue := 0 ;
  for i := 1 to 255 do
  begin
     DV := port[PA];
     gotoxy(27,15); writeln('Digital Voltage =', DV := 3);
     AV := (5/225)*DV;
     gotoxy(27,20); writeln('Analog Voltage =', AV:3:2,'V');
     delay(100);
     Ttrue := (39.919*AV+5.5948);
     gotoxy(27,22); writeln('Measure Temperature =', Ttrue:3,'deg C');
     delay(200);
  end;
end.
```

3) To do the instrument calibration, the electric current was supplied from a d.c. 5 V power supply through sample 1 and resistor1 (or resistor2 and sample 2). Then the sample was voltage dropped. This voltage (V) was supplied to ADC 0809 for conversion from analog voltage (AV) to digital voltage (DV). 74LS244 was used as a buffer. The voltage from this buffer was sent through port A of ET-PC8255 Card, slot and then to RAM. The voltage (DV) was read and displayed on the screen. The DV was conversed to AV. The sample temperature was increased with the electric furnace. To do the calibration, the true temperature (Ttrue) was read with commercial temperature apparatus (Union 305) with type K thermocouple as a temperature sensor and the dropped voltage on the resistor (AV) which relate to the sample was read from the valuê on the screen from 25 to 65 °C for the sample 1 and 25 to 85 °C for the sample 2. This data (Ttrue, AV) were recorded into the table and plotted with EXCEL. The Ttrue versus AV was obtained and then was written into this program. After RUN, computer will read the temperature (Tmeasure). Final calibration step, the Ttrue and Tmeasure were read, recorded and plotted to be bar graph for comparison. Finally, we obtained the temperature apparatus with computer displaying and the prepared sample as a temperature sensor.

3. Results

3.1 Sample Phase

X-ray diffraction patterns were shown in Figure 4.

Composition formula and sample phase from XRD patterns were shown in Table 1.

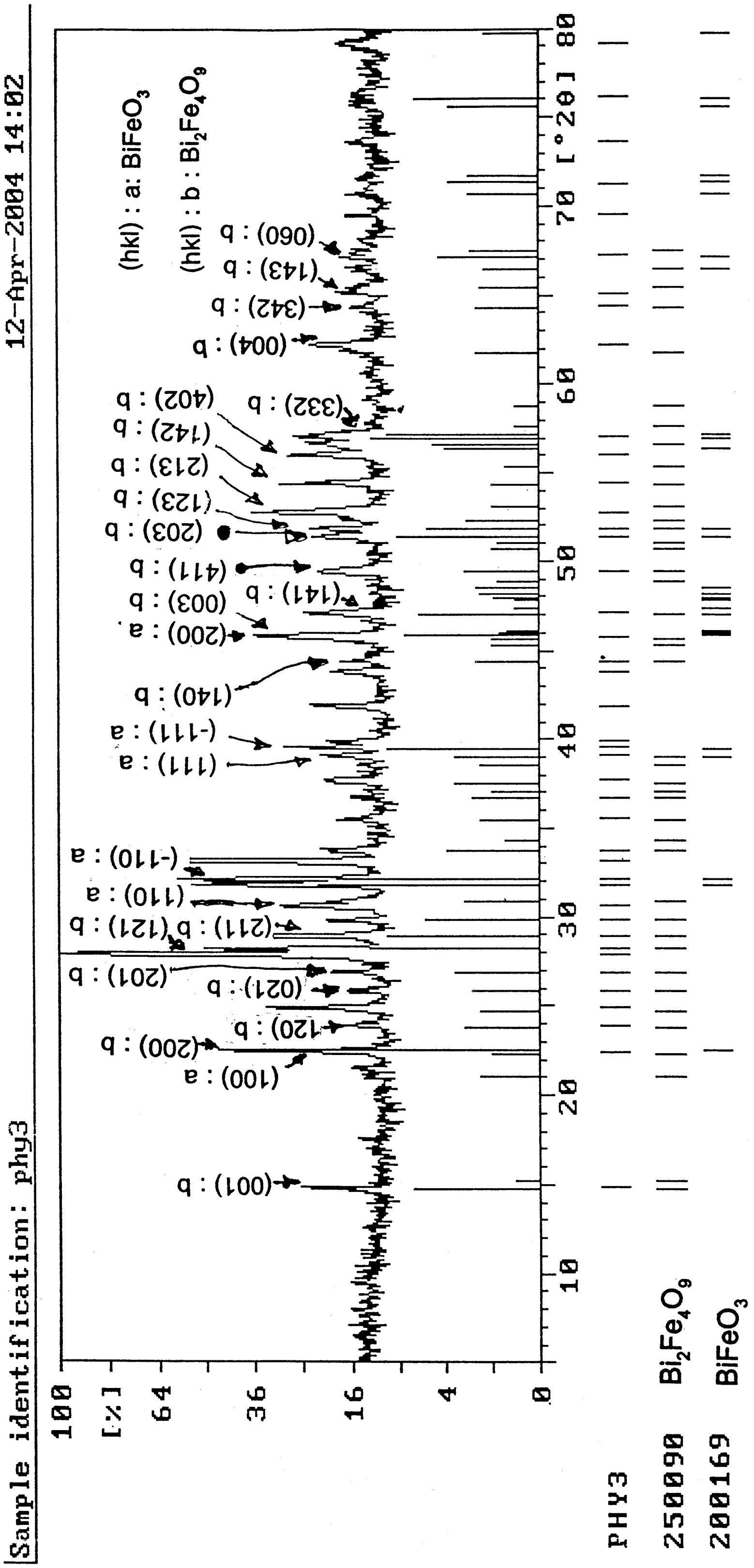

a. The sample 1 (Bi_2O_3+Fe_2O_3)

Figure 4. X-ray diffraction patterns of the samples.

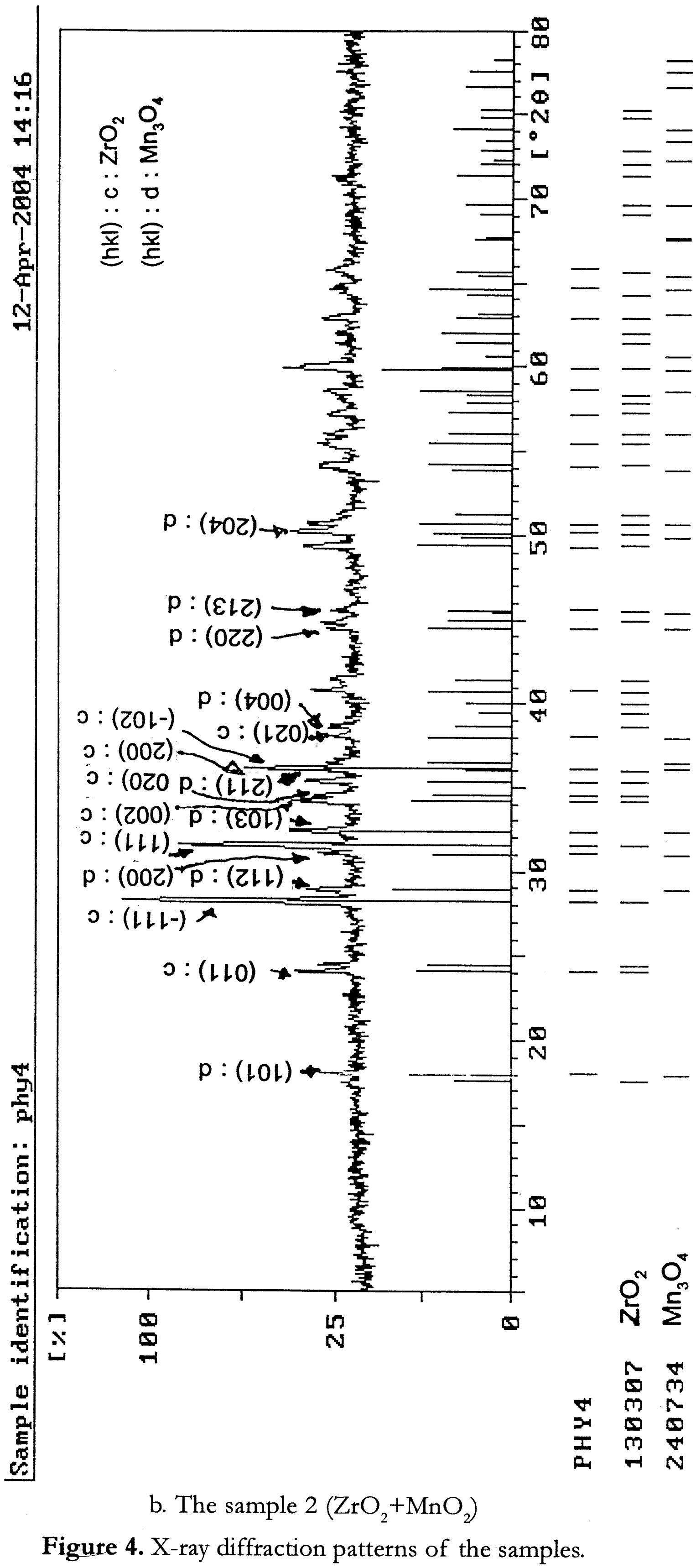

b. The sample 2 (ZrO_2+MnO_2)

Figure 4. X-ray diffraction patterns of the samples.

Table 1. Sample phase for the Bi_2O_3+Fe_2O_3 and ZrO_2+MnO_2 samples.

Sample No.	Composition formula	Sample phase from XRD
1	Bi_2O_3+Fe_2O_3	$BiFeO_3$, $Bi_2Fe_4O_9$
2	ZrO_2+MnO_2	ZrO_2, Mn_3O_4

2. The Resistance Versus Temperature Characteristics of the Samples

The resistance versus temperature relation of the samples from 25 to 200 °C were shown in Figure 5. The resistance of the sample 1 was increased as the temperature increasing or showed the PTC effect from 25 to 110 °C and the resistance was decreased as the temperature increasing or showed NTC effect from110 to 200 °C. But, the sample 2 showed PTC effect from 25 to 130 °C and NTC effect from 130 to 200 °C.

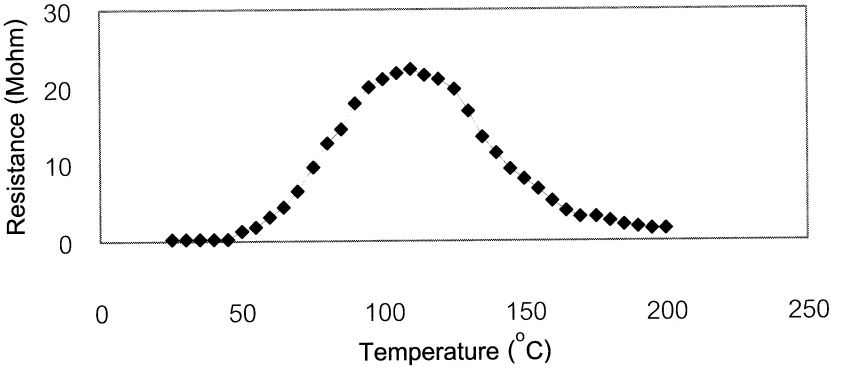

a. sample 1

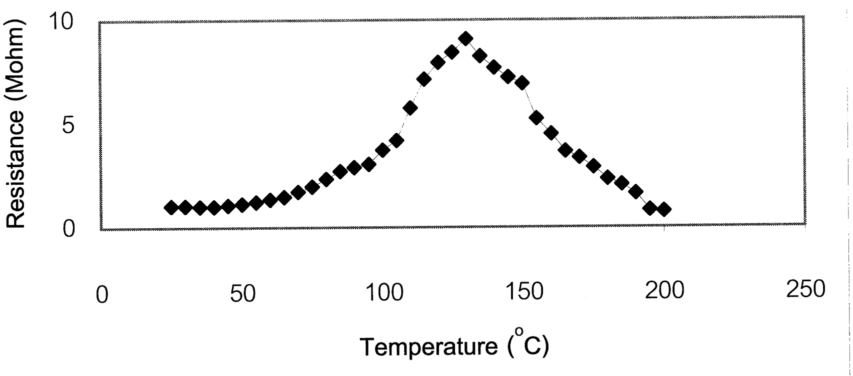

b. sample 2

Figure 5. The resistance versus temperature of the sample 1 : Bi_2O_3+Fe_2O_3 and sample 2 : ZrO_2+MnO_2.

3. The Constructed Temperature Apparatus with Computer Displaying and the Prepared Sample as a Temperature Sensor

The true temperature (Ttrue) and the voltage (AV) was shown in Figure 6 and correspond to the equation :

Sample 1 : $Ttrue = 77.723e^{-0.2255(AV)}$

Sample 2 : $Ttrue = 2.5837(AV)^2 + 9.9138(AV) + 2.5096$

The graphs a. and b. have different slope because of the different connection of load resistor and sample in a series form as setting for input sensor in this system.

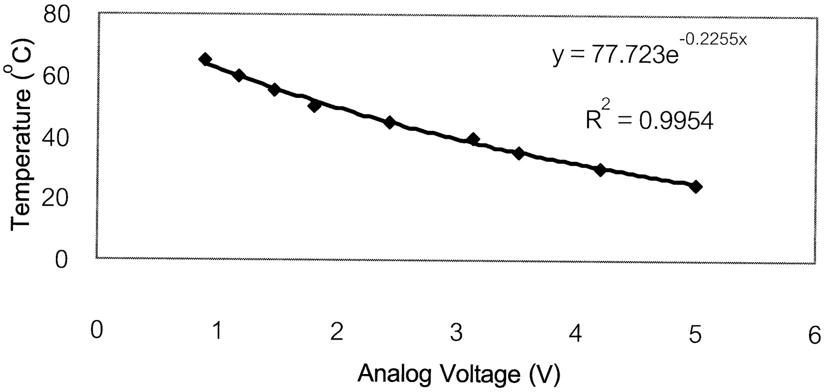

a. sample 1 (25-65 °C)

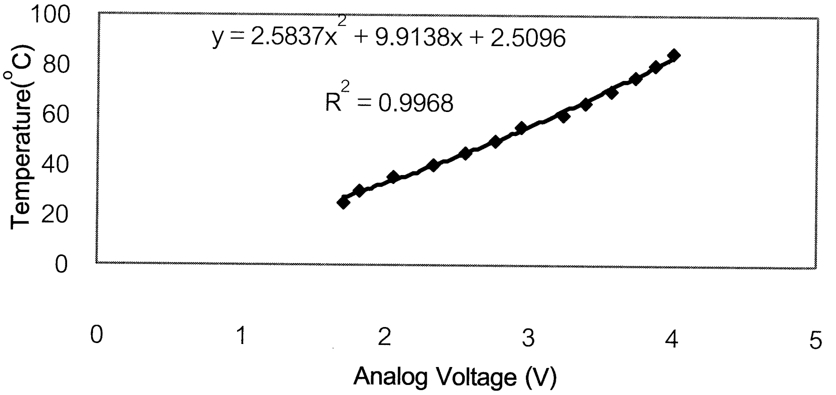

b. sample 2 (25-85 °C)

Figure 6. Temperature vs analog voltage of the Bi_2O_3+Fe_2O_3 and ZrO_2+MnO_2 samples.

This equation was used for calibration to use the prepared sample as a temperature sensor. Figure 7 showed the comparison between True temperature (Ttrue) and measure temperature (Tmeasure). From the picture, the sample 1 and 2 showed the physical properties of PTC thermistor and can be used as temperature from 25 to 65 °C and 25 to 85 °C.

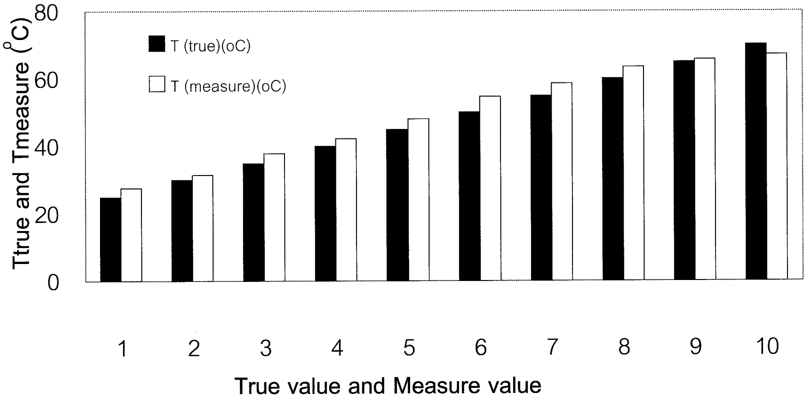

a. sample 1 (25-65 °C)

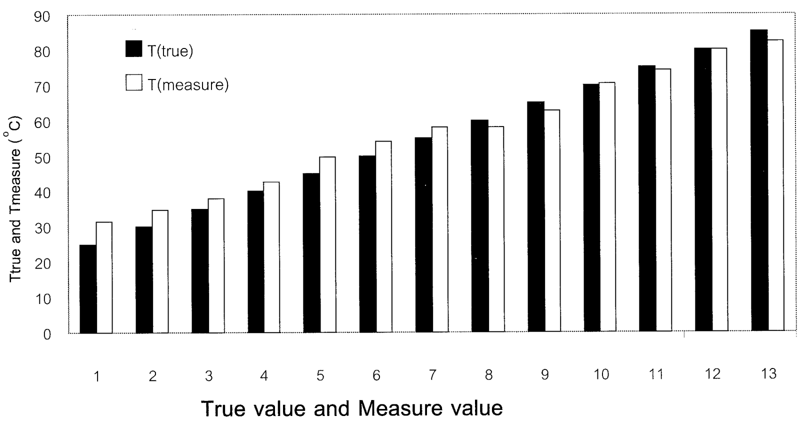

b. sample 2 (25-85 °C)

Figure 7. Comparison between true temperature (Ttrue) and measured temperature (Tmeasure) of the Bi_2O_3+Fe_2O_3 and ZrO_2+MnO_2 samples.

4. Discussion and Conclusion

The both samples were disc-shaped. The composition of the prepared sample were Bi_2O_3+Fe_2O_3 and ZrO_2+MnO_2. The sample 1 was the two phase materials which composed of $BiFeO_3$ and $Bi_2Fe_4O_9$. The sample 2 was the two phase materials which composed of ZrO_2 and Mn_3O_4. The MnO_2 was altered to be Mn_3O_4 due to the effect of firing.

The resistance of the sample 1 was to increase with increasing temperature. The sample exhibited PTC effect from 25 to 110 °C. The positive temperature coefficient of the resistance (α) was +183.24 %/°C in the 25 to 110 °C range. The relation between the resistance (R) and the temperature (T) corresponds to the equation : $R = 0.0031T^2-0.1007T - 0.4206$. But, the resistance of the sample was to decrease with increasing temperature from 110 to 200 °C. The sample exhibited NTC effect. The negative temperature coefficient of the resistance (a) was –1.16 %/°C in the 110 to 200 °C range. The relation between the resistance (R) and the temperature (T) corresponds to the equation : $R = 0.0029T^2 - 1.1696T + 117.67$. The maximum resistance was 22.24 MΩ at 110 °C.

The resistance of the sample 2 was to increase with increasing temperature. The sample exhibited PTC effect from 25 to 130 °C. The positive temperature coefficient of the resistance (a) was +7.08 %/°C in the 25 to 130 °C range. The relation between the resistance (R) and the temperature (T) corresponds to the equation : $R = 0.0012T^2-0.1118T + 3.4894$. But, the resistance of the sample was to decrease with increasing temperature from 130 to 200 °C. The sample exhibits NTC effect. The negative temperature coefficient of the resistance (α) was –1.36 %/°C in the 130 to 200 °C range. The relation between the resistance (R) and the temperature (T) corresponds to the equation : $R = 0.0007T^2 - 0.3647T + 44.385$. The maximum resistance was 9.08 MΩ at 130 °C.

The positive temperature coefficient of the resistance of the PTC material which made from $BaTiO_3$ was the value range from +10 to +100 %/°C [1-2]. When compared the PTC case, the a value of the sample 1 was higher than the $BaTiO_3$ and the sample 2 was lower than the $BaTiO_3$. The sample 1 was thermal- sensitive than the sample 2.

The both prepared samples showed PTC effect. This PTC effect was similar to that occurred in PTC effect in $BaTiO_3$ [1-2]. The ferroelectric effect had not been studied. The PTC effect in the Bi_2O_3+Fe_2O_3 and ZrO_2+MnO_2 samples were discovered in the first time at material physics laboratory, Department of Physics, Faculty of Science, Prince of Songkla University, Thailand. The samples was a very sensitive to the temperature in the PTC region. So, the samples can be used as temperature sensor which are suitable to do the learning and teaching work. The prepare samples and the temperature monitoring with computer system can measure the temperature in the range 25 °C to 65 °C (sample 1) and 25 °C to 85 °C (sample 2). The working temperature of this sensors are in the PTC region which are very sensitive to heat.

The characteristics of the thermistors which made from this two materials were :

1) The firing temperature is not high which use only the low temperature furnace.

2) The samples have a good electrical stability ($\Delta R/\Delta t$).

3) The samples were not responsive to the light.

4) The samples were very sensitive to heat.

5) The shape of the resistance versus temperature curves were smooth.

6) The samples can be used as a temperature sensor that display with the computer.

7) The samples are semiconducting ceramics because they exhibit thermal sensing property.

So, this PTC materials are important for electronic industrial application and further research.

ACKNOWLEDGEMENT

This investigation was supported by Prince of Songkla University (PSU) and The National Research Council of Thailand (NRCT), Thailand. The authors wish to thank Miss Putsadee Muhamud for XRD measurements and analysis.

REFERENCES

[1] Moulson A.J., and Herbert J.M., *Electroceramics*, Chapman & Hall, London, 1990.

[2] Relva B.C., *Ceramic materials for electronics*, second edition, New York : Mercel Dekker Inc., 1991.

[3] Dostert K., Applications of self-heated PTC thermistors to flow and quality of heat measurements, *Sensors and Actuators*,

1983 ; **3** : 159-167.
[4] Issa M.A.A., Electrical properties of polycrystalline PTCR barium titanate, *J. of Mater. Sci.*, 1992; **27** : 3685-3692.
[5] Miyayama M., Infrared sensing properties of positive temperature coefficient thermistors with large temperature coefficient of resistivity, *J. Mater. Sci.*, 1992; **27** : 127-132.
[6] Padmini P., Influence of Bi^{3+} ions in enhancing the magnitude of positive temperature coefficients of resistance in n-$BaTiO_3$ ceramics, *J. Mater. Sci., : Mater. In Elect.*, 1994; **5** : 203-209.
[7] Chang H., Electrical characteristics of $(Sr_{0.2}Ba_{0.8})TiO_3$ positive temperature coefficient of resistivity materials prepared by microwave sintering, *J. Appl. Phys.*, 1995; **78(1)** : 423-427.
[8] Wang D.J., Preparation and electrical properties of semiconducting strontium-lead titanate PTCR ceramics, *J. Mater. Sci. : Mater. In Elect.*, 1997; **8** : 271-276.
[9] Shibagaki S., Calcium-doping effect on temperature coefficients of dielectric constants in $SrTiO_3$ capacitors, *J. Mater. Sci.*, 1997; **32** : 1449-1453.
[10] Xue J., Uniform incorporation of sintering aids and MnO in PTC $BaTiO_3$ by liquid phase coating, *Ferroelectrics*, 1997; **195** : 137-140.
[11] Igor Z., Preparation of PTCR ceramics in the BaO-Nb_2O_5-TiO_2 system, *J. European Ceramic Society*, 1999; **19** :893-896.
[12] AI-Shahran A., Positive temperature coefficient in Ho-doped $BaTiO_3$ ceramics, *J. Physics and Chemistry of Solids*, 2000; **61** : 955-959.
[13] He Z., Strucural model of Cr/(Ba,Pb) TiO_3 positive temperature coefficient composite, *J. Mater. Sci. : Mater. In Elect.*, 2000; **11** : 235-238.
[14] Meier K., PTC thermistor heating elements, *Appliance*, 2001; **58** : 64-66.
[15] Jingchang Z., Study on the properties of (Y, Mn) co-doped $Sr_{0.5}Pb_{0.5}TiO_3$ thermistors, *Materials Science and Engineering B.*, 2002; **94** : 202-206.
[16] Srinivas A., Processing and study of dielectric and ferroelectric nature of $BiFeO_3$ modified $SrBi_2Nb_2O_9$, *Ceramics International*, 2004; **30(7)** : 1427-1430.
[17] Khozeev D.F. , Spin modulation of 57Fe NMR frequency and relaxation in $BiFeO_3$, Physica B : Condensed Matter, *Proc. 23rd International Conference on Low Temperature Physics*, 2003; **329-333** : 848-849.
[18] De Sitter J., On the magnetic properties of the basic compounds in the Fe_2O_3-Bi_2O_3 system, *Physica B+C*, 1977; **86-88(2)** : 919-920.
[19] Groult D., 3.1 GeV-Xenon ion latent tracks in $Bi_4Fe_2O_9$: High-resolution electron microscope observations, *J. Solid State Chemistry*, 1988; **76(2)** : 260-265.
[20] Poghossian A.S., Bismuth ferrites: New materials for semiconductor gas sensors, *Sensors and Actuators B : Chemical*, 1991; **4(3-4)** : 545-549.
[21] Kostiner E., Mossbauer effect study of $Bi_2Fe_4O_9$, *J. Solid State Chemetry*, 1971; **3(2)** : 186-189.
[22] Liangrong L., Synthesis and characterization of monoclinic ZrO_2 nanorods by a novel and simple precursor thermal decomposition approach, *Solid State Communications*, 2003;**127(9-10)** : 639-643.
[23] Chang Y.Q., Synthesis and characterization of Mn_3O_4 nanoparticles, *J. Crystal Growth*, 2004; **264(1-3)** : 232-236.